

PACS numbers: 42.68.Ay; 42.68.Jg; 42.65.Re
DOI: 10.1070/QE2015v045n02ABEH015445

Modelling of radiative transfer by the Monte Carlo method and solving the inverse problem based on a genetic algorithm according to experimental results of aerosol sensing on short paths using a femtosecond laser source

G.G. Matvienko, V.K. Oshlakov, A.N. Stepanov, A.Ya. Sukhanov

Abstract. **We consider the algorithms that implement a broadband ('multiwave') radiative transfer with allowance for multiple (aerosol) scattering and absorption by main atmospheric gases. In the spectral range of 0.6–1 μm, a closed numerical simulation of modifications of the supercontinuum component of a probing femtosecond pulse is performed. In the framework of the algorithms for solving the inverse atmospheric-optics problems with the help of a genetic algorithm, we give an interpretation of the experimental backscattered spectrum of the supercontinuum. An adequate reconstruction of the distribution mode for the particles of artificial aerosol with the narrow-modal distributions in a size range of 0.5–2 mm and a step of 0.5 mm is obtained.**

Keywords: *radiation, atmosphere, transfer, aerosol, lidar, femtosecond laser, supercontinuum, inverse problem, genetic algorithm, Monte Carlo method.*

1. Introduction

Currently, one of developing directions of atmospheric optics and lidar sensing is the use of pulsed laser sources of femtosecond duration. Propagation of a high-power femtosecond (FS) pulse in the atmosphere is accompanied by a number of different processes, including ionisation, single and multiphoton absorption, and Rayleigh, Raman and hyper-Raman scattering. The greatest interest for the problems of atmospheric sensing is the use of supercontinuum (SC) radiation arising during filamentation of a high-power FS probing pulse: a fraction of the pulse energy is distributed over a wide (relative to the laser wavelength) spectral range both in the Stokes and anti-Stokes spectral regions. Generally accepted is the following [1–11]: if the pulse power exceeds a certain threshold (3–3.5 GW for air), a nonlinear addition to the refractive index of a propagation medium becomes essential. The pulse enters into the self-focusing conditions, the intensity increases, the processes of multiphoton absorption and tunnelling ionisation become implemented and a plasma is formed at the pulse forefront. The incoming pulse, interacting with the plasma formation, is partly dissipated, but remains under the self-focusing conditions as long as the 'excess' energy is not exhausted. Filamentation is observed: the pulse path is visually registered in the form of a bright glowing thread (filament). At the same time, generation of conical SC emission occurs – the spectral energy, predominantly in the anti-Stokes region, is distributed within the cones, the apexes of which are located in the filamentation zone, and with a clearly expressed angular distribution according to the rule: the shorter the wavelength, the greater the angle at the cone apex. In the Stokes region of the spectrum, the energy is concentrated in the paraxial zone of the spatially compressed pulse. These effects can be widely used for quantitative and qualitative assessment of atmospheric parameters. Examples are the results of the international research project Teramobile, which uses a mobile femtosecond lidar system of terawatt power [1–7].

Along with the development of methods for atmospheric sensing by means of ultrashort pulses (USPs), methods for solving the inverse problems of FS atmospheric optics are being developed, among which we can distinguish the methods for numerical simulation of propagation of FS pulses. A separate task is the interpretation of atmospheric sensing by those pulses, which have experienced filamentation, with the use of SC radiation. Without claiming for completeness of our review, we point out that in the last ten years the scientific teams of the institutes of Russian Academy of Sciences have made a sufficiently large contribution to this area. The authors of [8–15] consider typical results of experimental and numerical studies on FS radiation propagation in the atmosphere and aerosol cloud. In Refs [8, 9] the authors formulate the lidar equation describing the atmospheric sensing by FS pulses; herewith the sensing path is conventionally divided into linear and nonlinear parts. The effect of splitting of FS pulses in the linear transfer regime has been numerically investigated, and the effectiveness of the use of white light lidars for sensing the optical and microphysical parameters of an aerosol cloud have been analysed. The methodology of modelling the propagation of a signal with a wide spectrum and of solving the inverse problems of atmospheric optics as applied to FS atmospheric optics is presented in [16–20]. Numerical studies on the possibility of using white light lidars on short atmospheric paths in the problems of reconstruction of particle size distribution functions have been carried out. The reconstruction and modelling methods that have been suggested previously are generally related to the separate (four) wavelengths falling into the transparency window of the atmosphere, but the results have not been supported by full-scale experiments.

G.G. Matvienko, V.K. Oshlakov, A.Ya. Sukhanov V.E. Zuev Institute of Atmospheric Optics, Siberian Branch, Russian Academy of Sciences, pl. Akad. Zueva 1, 634021 Tomsk, Russia; e-mail: mgg@iao.ru, ovk@iao.ru, say@iao.ru;
A.N. Stepanov Institute of Applied Physics, Russian Academy of Sciences, ul. Ulyanova 46, 603950, Nizhnii Novgorod, Russia

Received 3 March 2014; revision received 3 September 2014
Kvantovaya Elektronika **45** (2) 145–152 (2015)
Translated by M.A. Monastyrskiy

This paper describes the algorithms that are based on the Monte Carlo method and implement a broadband ('multi-wave') radiative transfer with allowance for multiple (aerosol) scattering and absorption by main atmospheric gases. As an example of interpretation of the experimental results on aerosol sensing, a problem of reconstruction of the distribution mode of aerosol particles in sizes using a genetic algorithm is being solved. For this purpose, an aerosol generator (ethylene glycol) with a known narrow-mode original distribution is used in a full-scale experiment. The artificial aerosol cloud is exposed to SC radiation arising in propagation of a FS pulse along the atmospheric path.

2. Full-scale experiment

A full-scale experiment on lidar sensing of the artificial aerosol cloud on a short (85 m) atmospheric path was performed using a femtosecond stand at the Institute of Applied Physics (Nizhnii Novgorod) [21] with the following FS system parameters: radiation wavelength of 800 nm, pulse duration about 50 fs, pulse energy of 10–14 mJ and pulse repetition rate of 1 kHz. The origin of pulse filamentation was located at a distance of 5–7 m from the output mirror of the laser system.

Engineering characteristics of the receiving optical system are as follows: Newtonian telescope (parabolic mirror with a diameter of 200 mm and a focal length of 70 cm), field diaphragm (single-wire optical fibre designed to transmit the radiation spectrum into the spectrometer with a diameter of 1000 mm). As a recorder use was made of a miniature high-speed high-resolution HR4000 spectrometer (Ocean Optics). The time of accumulation of photoelectrons was synchronised with the repetition rate of probing pulses.

As a source of artificial aerosol, a generator of aerosol particles based on ethylene glycol with a modal particle diameter of 1 μm and a small width of the mode of the particle size distribution function was used. The refractive index of this substance in the wavelength range of 400–1000 nm varied from 1.5 to 1.4, which best corresponds to the fraction of aerosol based on sea-salt particles.

Due to the specific character of the problem of aerosol formation sensing on a short (horizontal) atmospheric path, a biaxial lidar scheme with the following characteristics was chosen: lidar base (the distance between the optical axes of the transmitter and receiver) – 8.2 m, scattering angle (with regard to the distance to the point of sensing equal to 85 m) – approximately 174.5°. This excluded the possibility of recording high-intensity signals both from pre-filamentation and filamentation regions. The scheme of sensing is presented in Fig. 1.

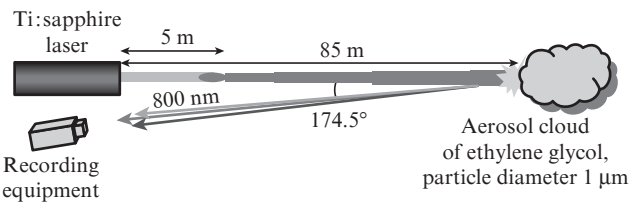

Figure 1. Scheme of the experiment carried out at the stand of the Institute of Applied Physics, RAS. Path markings: 5 m is the zone of self-focusing, filamentation and SC generation; 85 m is the zone of SC propagation; 174.5° is the scattering angle.

In this experiment, the nonlinearity of a propagation medium (the atmosphere) is manifested: the conical SC emission is generated in the air on initial part of the path. The image of coloured rings on the screen located perpendicular to the axis of radiation propagation is recorded with a digital video camera. According to the results of processing of the images of the angular distribution of SC radiation on the screen (Fig. 2a), the divergence angles of SC spectral components (Fig. 2b) and the position of the point of its generation

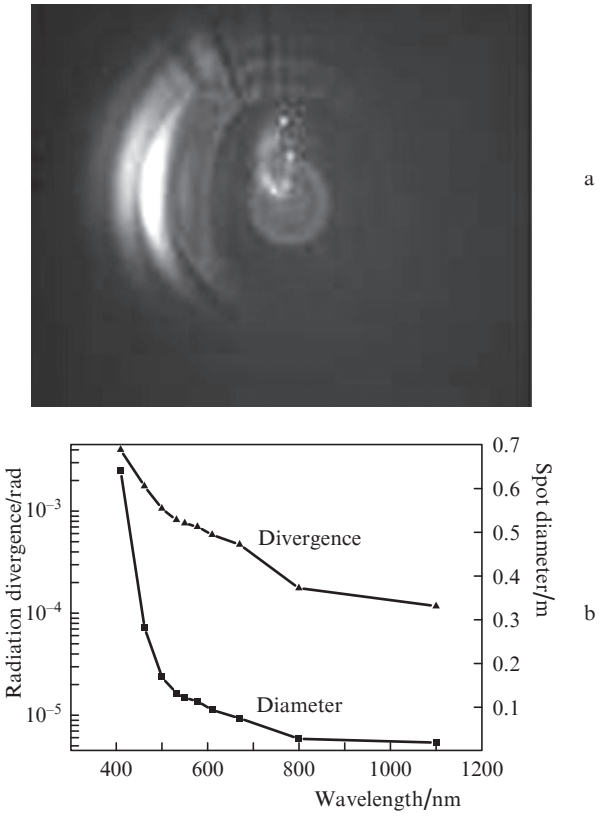

Figure 2. (a) Spectral-angular distribution of the radiation of conical emission and (b) spectral SC characteristics calculated according this distribution.

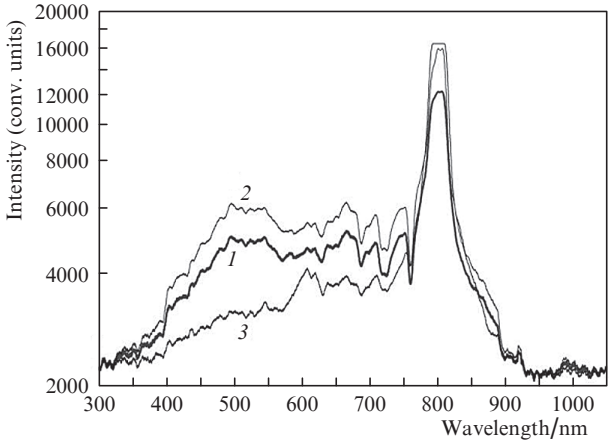

Figure 3. Spectra of backscattered signals of supercontinuum (distance to the point of scattering is 85 m, scattering angle is 174.5°): the average over 100 spectra of SC backscattering signals (*1*) and maximum (*2*) and minimum (*3*) energy transfer into SC by a single pulse.

on the path are estimated. The data obtained coincide basically with the data from [11, 12].

The SC radiation was recorded by a spectrometer at the path end (hereinafter, 'SC spectrum') and at the point of receiving the backscattered radiation of the SC. As a result of the experiment conducted with the use of a lidar layout (see Fig. 1), the signals of backscattered SC radiation from the artificial aerosol (ethylene glycol) with a particle diameter of 1 mm were received (Fig. 3).

3. Processing of the results of a full-scale experiment and numerical simulation of the experiment

In order to obtain information about the size distribution of aerosol particles, real spectra of the backscattered SC signals were processed. In the simulation, we assumed that, after taking into account the energy losses, filamentation, SC generation and related effects, the result of sensing of the path sections located behind the filamentation region can be described in terms of the linear equations of sensing with the use of the methodology developed for multi-frequency lidar sensing [22]. In solving the problem of reconstruction of the parameters of particle size distribution in the scattering volume, concomitant experimental data were used.

The linear propagation of radiation in a medium is described by the nonstationary integro-differential Boltzmann equation, which in three-dimensional space can be represented as follows:

$$v^{-1}\frac{\partial I(r,w,t,\lambda)}{\partial t} + w\nabla I(r,w,t,\lambda) = -\sigma(r,t,\lambda)I(r,w,t,\lambda)$$

$$+\frac{1}{4\pi}\int_{\Lambda}\int_{2\pi} I(r',w',t,\lambda')\int_{t}^{t^*} G(r,w',w,t',\lambda')\,\mathrm{d}t'\mathrm{d}w'\mathrm{d}\lambda'$$

$$+ I_0(r,w,t,\lambda), \qquad (1)$$

where

$$G(r,w',w,t,\lambda) = G_{\mathrm{M}}(r,w',w,t,\lambda'=\lambda) + \int_{\Lambda} G_{\mathrm{R}}(r,w',w,t,\lambda')\,\mathrm{d}\lambda';$$

$I(r,w,t,\lambda)$ is the radiation intensity with a wavelength λ at point r in the direction $w(a,b,c)$ at the time moment t; $I_0(r,w,t,\lambda)$ is the function of sources; v is the absolute velocity of particles in a medium; $G_{\mathrm{M}}(r,w',w,t,\lambda'=\lambda)$ is the volumetric ratio of the directional monochromatic elastic scattering in the direction $\vartheta = w'w$; $G_{\mathrm{R}}(r,w',w,t,\lambda')$ is the volumetric coefficient of the broadband elastic and inelastic scattering; and $\sigma(r,t,\lambda) = \sigma_{\mathrm{a}}(r,t,\lambda) + \sigma_{\mathrm{s}}(r,t,\lambda) + \alpha_{\mathrm{mol}}(r,t,\lambda)$ is the absorption coefficient (σ_{a}), the scattering coefficient (σ_{s}) of a dispersion medium and the coefficient α_{mol} of molecular absorption.

Various methods for obtaining the analytical solution of this transfer equation exist, and the Monte Carlo method can be attributed to rather effective ones. Besides, this approach has been consistently developed in our previous papers [8, 9, 14, 16–20].

Among numerous modifications of the Monte Carlo method, the method of local evaluation is effective in the problems of optical location. In the framework of this method, the expression for statistical evaluation of the radiation flux in the detector region $D_{ij} = \Omega_i T_j$ and within the spectral range takes the form [23]

$$I_{\Delta\lambda}(r^*) =$$

$$\sum_{n=0}^{N} q_n \frac{\exp[-\tau(r_n,r^*)]\,g(\mu^*,r)\,P^*_{\Delta\lambda}(r_n,r^*,\Delta\lambda)}{2\pi\,|r_n - r^*|^2}\Delta_i(s^*)\Delta_j(t^*). \quad (2)$$

Here, $g(\mu^*,r,\lambda)$ is the generalised indicatrix of scattering, normalised to unity; $\Delta_i(s^*)$ and $\Delta_j(t^*)$ are the indicators of the regions Ω_i and T_j; q_n is the statistical weight of the photon that compensates for the fictitious character of the transitions $(x_n \to x^*)$;

$$P^*_{\Delta\lambda}(r_n,r^*,\Delta\lambda) = (\Delta\lambda)^{-1}\int_{\Delta\lambda}\exp[-\tau_{\mathrm{mol}}(r_n,r^*,\lambda)]\,\mathrm{d}\lambda$$

$$= (\Delta\lambda)^{-1}\int_{\Delta\lambda}\exp\left[-\int_0^{|r_n-r^*|}\alpha_{\mathrm{mol}}(\lambda,r')\,\mathrm{d}r'\right]\mathrm{d}\lambda \qquad (3)$$

is the transmittance function; and τ_{mol} is the optical thickness conditioned by molecular absorption.

In this case, the canonical algorithm of local evaluation for the monochromatic regime is complemented by the factor (3) that requires additional calculations. Spectral absorption in the range of the photon path between the successive random collisions $\{r_n\}$, $n = 0,1,2,...$ is taken into account by transformation of the statistical weights

$$q_{n+1} = q_n P^n_{\Delta\lambda}(r_n,r_{n+1},\Delta\lambda),\ n = 0,1,2,..., \qquad (4)$$

where

$$P^n_{\Delta\lambda}(r_n,r_{n+1},\Delta\lambda) = (\Delta\lambda)^{-1}\int_{\Delta\lambda}\exp\left[-\int_0^{|r_{n+1}-r_n|}\alpha_{\mathrm{mol}}(\lambda,r')\,\mathrm{d}r'\right]\mathrm{d}\lambda. \quad (5)$$

The optical aerosol model includes the coefficients of optical interaction for ethylene glycol calculated by Mie theory with allowance for the refractive indices of the substance in the linear regime of SC radiation propagation. It is assumed that the scattering coefficient of aerosol is 2–10 times greater than the background values (0.05–0.1 km^{-1}).

The data on molecular absorption were obtained from the HITRAN database. In the ultraviolet and visible wavelength regions, the absorption cross sections for O_3, Cl_2, NO_2, SO_2 and the parameters of absorption lines were used to calculate the absorption coefficients in the approximation of the Voigt line shape. We have taken into account the following factors: absorption of H_2O in the ranges of 410–450 and 960–980 nm and in the region of 770 nm; absorption of NO_2 in the range of 300–600 nm (though the absorption of background concentrations in NO_2 can be considered insignificant for short paths, NO_2 concentration in urban conditions significantly increases); and absorption of O_3 in a region less than 350 nm and in the range of 500–700 nm (this absorption may become noticeable with a possible increase in the concentration of O_3).

As a model describing the distribution of gas components, we have chosen the model developed at the Institute of Atmospheric Optics, Siberian Branch of the RAS [24] and the updated gas model of the atmosphere [25], which is separated

into three layers: lower troposphere (0–5 km), upper troposphere (up to 12 km) and stratosphere (12–35 km). The experiment we analyse here was carried out in the conditions of lower troposphere. The aerosol background model was formed on the basis of papers [26–29] as a model of oceanic aerosols with coarsely dispersed (sea salt and mineral particles), accumulative (mineral particles and soil aerosol), and transitive (water-soluble and mineral particles, soot) fractions [28]. As particle size distribution functions we consider the lognormal distribution functions and the fractions given in Table 1.

Table 1. Main aerosol fractions.

Aerosol fraction	N/cm^{-3}	r_m/μm	σ
Insoluble soil and organic aerosols	0–2	0.471	2.51
Water-soluble aerosol	0–28000	0.0212	2.24
Soot particles	0–100000	0.0118	2
Transitive fraction	0–270	0.07	1.95
Accumulative fraction	0–30	0.39	2.0
Coarsely dispersed fraction	0–0.14	1.9	2.15
Fine particles of sea salt	0–150	0.209	2.03
Large particles of sea salt	0–0.04	1.75	2.03

In this case, the boundary atmospheric layer is only considered; therefore, we omit here the description of the altitude distribution of the particle concentration.

The numerical experiment in the framework of the Monte Carlo method represents modelling of the biaxial lidar scheme. In accordance with the scheme of the full-scale experiment, Krekov's aerosol optical model that had been used previously was complemented by the scattering angle of 174.5° with allowance for the indicatrices of scattering for the molecular and aerosol atmosphere.

The coefficients of optical interaction were calculated using Mie theory. Scattering indicatrices and coefficients of scattering and attenuation played the role of calculated parameters. The size distribution of particles of the background aerosol was described in terms of the lognormal distribution with the parameters taken from Table 1:

$$\frac{\mathrm{d}N_i(r)}{\mathrm{d}r} = \frac{N_i}{\sqrt{2\pi}\, r \lg\sigma_i \ln 10} \exp\left[\frac{1}{2}\left(\frac{\lg r - \lg r_{mi}}{\lg\sigma_i}\right)^2\right], \tag{6}$$

where r_{mi} is the modal radius of the particle distribution; N_i is the concentration of the ith fraction; and σ_i is the rms deviation.

The optical model of an artificial aerosol cloud was calculated using a Gaussian distribution so that the scattering according to the background model was exceeded by 2–5 times. The distribution mode for different cases constituted 0.5 – 2 μm, with the half-width of the mode equal to 0.005 μm.

4. Inverse problem solution

In our case, we consider the problem of seeking the size distribution functions of particles as applied to the artificial aerosol formation. It is assumed that the majority of particles have an approximately equal radius. The problem is reduced to optimisation of a functional representing an implementation of the method of least squares, and thus to minimisation of the difference between the spectrum of backscattered SC radiation, obtained experimentally, and the model spectrum relevant to a given particle size distribution obtained via the genetic algorithm:

$$\sum_{i=1}^{n} (I_{\exp}(\lambda_j) - aI_{\mathrm{mod}}(\lambda_j))^2 \to \min, \tag{7}$$

where $I_{\exp}(\lambda_j)$ is the experimental spectrum and $aI_{\mathrm{mod}}(\lambda_j)$ is the model spectrum multiplied by a scaling factor.

It should be noted that, in order to test the results of modelling based on the use of the genetic algorithm, we used as $I_{\exp}(\lambda_j)$ the spectrum obtained in modelling by the Monte Carlo method. The model representation of the signal takes into account only single scattering of photons and, with allowance made for parameters of full-scale experiment, takes the form

$$I_{\mathrm{mod}}(\lambda_j) = \frac{I(\lambda_j) D_{\lambda j} A}{R_{85}^2} \int_0^{\Delta} G(h + R_{85}) \exp\left\{-\int_{R_{85}}^{R_{85}+h} \beta(\lambda_j, h')\,\mathrm{d}h' \right.$$
$$\left. - \int_{R_{85}}^{R_{85}+h/\cos(174.5^\circ)} \beta[\lambda_j, h' |\cos(174.5^\circ)|]\,\mathrm{d}h' \right\} \beta_{174.5}(\lambda_j, h + R_{85})\,\mathrm{d}h$$
$$\times \exp\left\{-\int_0^{R_{85}/\cos(174.5^\circ)} \beta_{\mathrm{ext}}^{\mathrm{a+m}}[\lambda_j, h\,|\cos(174.5^\circ)|]\,\mathrm{d}h \right.$$
$$\left. - \int_{R_5}^{R_{85}} \beta_{\mathrm{ext}}^{\mathrm{a+m}}(\lambda_j, h)\,\mathrm{d}h \right\}. \tag{8}$$

Here, $D_{\lambda j}$ is the transmittance of the receiving channel at the wavelength λ_j; A is the receiving aperture area; $G(h)$ is the geometric factor; R_{85} is the distance from the receiver to the aerosol cloud; $I(\lambda_j)$ is the radiation intensity of the conical emission at the wavelength λ_j; $\beta_{174.5}(\lambda_j, h)$ is the coefficient of scattering at the angle 174.5° in the receiver direction, conditioned by artificial aerosol and molecular atmosphere; $\beta_{\mathrm{ext}}^{\mathrm{a+m}}(\lambda_j, h)$ is the molecular and aerosol attenuation on the path; Δ is the depth of the aerosol cloud; and $I(\lambda_j)$ is the original SC spectrum.

The coefficients of scattering and attenuation at the angle of 174.5° can be represented as follows:

$$\beta(\lambda_j, h) = \int_{r_1}^{r_2} \varphi(r)\beta(\lambda_j, h, r)\,\mathrm{d}r + \beta_{\mathrm{atm}}(\lambda_j, h),$$
$$\beta_{174.5}(\lambda_j, h) = \int_{r_1}^{r_2} \varphi(r)\beta_{174.5}(\lambda_j, h, r)\,\mathrm{d}r + \beta_{\mathrm{atm},174.5}(\lambda_j, h), \tag{9}$$

where $\beta(\lambda_j, h, r)$ and $\beta_{174.5}(\lambda_j, h, r)$ are the coefficients of attenuation and scattering at the angle of 174.5° for a particle of radius r;

$$\varphi(r) = M\left\{\alpha \exp\left[-\frac{(r - r_1)^2}{2g_1^2}\right] + \exp\left[-\frac{(r - r_2)^2}{2g_1^2}\right]\right\} \tag{10}$$

is the size distribution function of particles, represented as a sum of two Gaussian functions normalised by the coefficients $\alpha \in [0, 1]$ and M (normalisation factor of the distribution density per unity).

To solve problem (7), the genetic algorithm [16, 19, 20] is applied. The generally recognised disadvantage of genetic algorithms is slow convergence to the solution and large time of operation, which is caused by the need of multiple calcula-

tions of the selection function. With some simplifications, functional (7) is transformed into a fitness function; in particular, it is assumed that the coefficients of scattering and attenuation do not change along the sensing path, and the geometrical factor is equal to 1:

$$f(X) = \sum_{i=1}^{n} \Big\{ I_{\mathrm{br}}(\lambda_j) - aI_{\mathrm{sc}}(\lambda_j) \times \Big[b \int_{r1}^{r2} \varphi(r', M, \alpha, \bar{r}, \bar{g}) \beta_{174.5}(r, \lambda_j)\, \mathrm{d}r' + \beta_{174.5}^{\mathrm{a+m}}(\lambda_j) \Big] \times \Big[\frac{1}{2\beta(\lambda_j)} [1 - \exp(-2\beta(\lambda_j)\Delta)] \Big] \times \exp\Big[-2 \int_0^{85} \beta_{\mathrm{ext}}^{\mathrm{a+m}}(\lambda_j, h)\, \mathrm{d}h + \int_0^{5} \beta_{\mathrm{ext}}^{\mathrm{a+m}}(\lambda_j, h)\, \mathrm{d}h \Big] \Big\}^2 \times [I_{\mathrm{br}}(\lambda_j)^2]^{-1}, \quad (11)$$

where $f(X)$ is the fitness function dependent on the vector of the sought-for parameters $X = [a, b, \alpha, \Delta, \bar{r}, \bar{g}]$; a is the scale parameter of the signal; b is the coefficient of contribution to artificial aerosol scattering at the angle of 174.5°, which actually takes into account both relative contribution of the atmospheric component in comparison with the molecular and aerosol components, and the concentration of ethylene glycol particles; $\bar{r}$, $\bar{g}$ are the vectors of modes and half-widths of the Gaussian density distribution; M is the normalisation factor of the density distribution per unity; $\beta_{174.5}(r, \lambda_j)$ is the coefficient of scattering at the appropriate angle for an ethylene glycol particle with radius r; $\beta_{174.5}^{\mathrm{a+m}}(\lambda_j)$ is the coefficient of total scattering by aerosol and molecular atmosphere; $\beta_{\mathrm{ext}}^{\mathrm{a+m}}(\lambda_j, h)$ is the attenuation coefficient;

$$\beta(\lambda_j) = \int_{r1}^{r2} \varphi(r', M, \alpha, \bar{r}, \bar{g}) \beta(r, \lambda_j)\, \mathrm{d}r' + \beta_{\mathrm{atm}}(\lambda_j)$$

is the attenuation in the cloud; $I_{\mathrm{sc}}(\lambda_j)$ and $I_{\mathrm{br}}(\lambda_j)$ are the SC and backscattered signal spectra with the transmittance taken into account; and $\beta_{\mathrm{atm}}(\lambda_j)$ is the atmospheric background attenuation.

The experimental spectrum obtained at the path end at the distance of 85 m from the source was taken as an original SC spectrum, which was then corrected with regard to model transmittance along the path and used to obtain the probability of propagation of a hypothetical photon at a given wavelength.

The effect of conical SC emission generation was taken into account in modelling. Angular divergences of the spectral components were obtained from the analysis of experimental coloured images of the spectral-angular distribution of radiation of conical emission (Fig. 2). The values of angular divergences were used to estimate the position of the SC generation point on the path and to determine the propagation direction of an initiating hypothetical photon at a given wavelength.

The Gaussian distribution is chosen as the original particle size distribution because rather narrow single-mode spectra are considered. Because the calculation of such a function is time-consuming, the dependences of scattering on the wavelength and particle radius were calculated beforehand to speed up the calculation process. Besides, the integral of averaging over the distribution function was calculated in the mode vicinity only. As a result, the calculation time on the modern processors without parallelisation was reduced to 1 h.

The model values of optical coefficients are used for the coefficients of atmospheric attenuation and scattering at the angle of 174.5°. It is herewith assumed that the behaviour of these coefficients changes in scale (through the use of the coefficients b and a), rather than over the spectrum. The value $(2\beta(\lambda_j))^{-1}[1 - \exp(-2\beta(\lambda_j))\Delta]$ is almost constant over the spectrum in the range of 400–1000 nm, but, in order to take this value into account, the Δ parameter is taken between 0.1–2 m.

The model backscattering spectra for the conditions corresponding to the actual experiment were obtained using the Monte Carlo method and genetic algorithm. In the genetic algorithm, in order to reconstruct the parameters of the particle size distribution, representation (8) was used as a model signal spectrum in the single-scattering approximation. The backscattering spectra of SC radiation for a given set of parameters of the particle size distribution were monitored on the basis of best convergence either to the model spectrum obtained by the Monte Carlo method, or to the experimental spectrum. After positive evaluation of the results obtained for the signals with a wide spectrum on the basis of the genetic algorithm, the particle size distribution was reconstructed by means of the interpretation of experimental results with the use of *a priori* information about the distribution mode. In this case, the genetic algorithm enables a wider and more flexible change of the conditions of solving the inverse problem compared to other methods.

Below we compare the model spectra obtained by the Monte Carlo method and genetic algorithm for the particles of different sizes. In solving problem (7), the backscattered signal spectra in the range of 0.65–0.77 μm and 0.85–0.96 μm were taken into account. These limitations are due to the fact that, in the experimental spectra obtained, the signals have a too large signal-to-noise ratio in the vicinity of the laser radiation wavelength, whilst this ratio is too small at the edges of the supercontinuum glow.

The continuous dark line in Fig. 4 shows the spectrum reconstructed according to the genetic algorithm by fitting the parameters of the vector $X = [a, b, \alpha, \Delta, \bar{r}, \bar{g}]$ to the model spectrum obtained by the Monte Carlo method for different modal particle sizes (in Fig. 4 this spectrum is represented by the tone line and is noisy). It can be seen that the spectrum obtained using the genetic algorithm exactly reproduces the shape of the model signal obtained by the Monte Carlo method. In this case, the noises in the model spectrum (at a given noise level) do not greatly affect the reconstruction accuracy of the 'narrow' (0.5–2 μm) mode. Vertical lines restrict the spectral range of modelling: as stated above, the spectral ranges with a too large and too small signal-to-noise ratio in the experimental spectra are excluded from the calculations. In average over the spectrum, this ratio was equal to 30 at the minimum value 0.5.

In Figs 4c and 4d, a spectrum of the original signal irradiating the aerosol formation (SC spectrum) is added. One can see the way the spectra incident and scattered from clouds, recorded in the experiment, are transformed. The absolute amplitude of these spectra are normalised so that it is possible to put them on one and the same drawing.

It should be noted that, for the particles of 2 μm radius, the main difference in the shapes of the spectra obtained by two methods is observed at long wavelengths. The shapes of the spectra for the particles of 0.5 μm radius are virtually unchanged, and this quite correlates with spectral behaviour

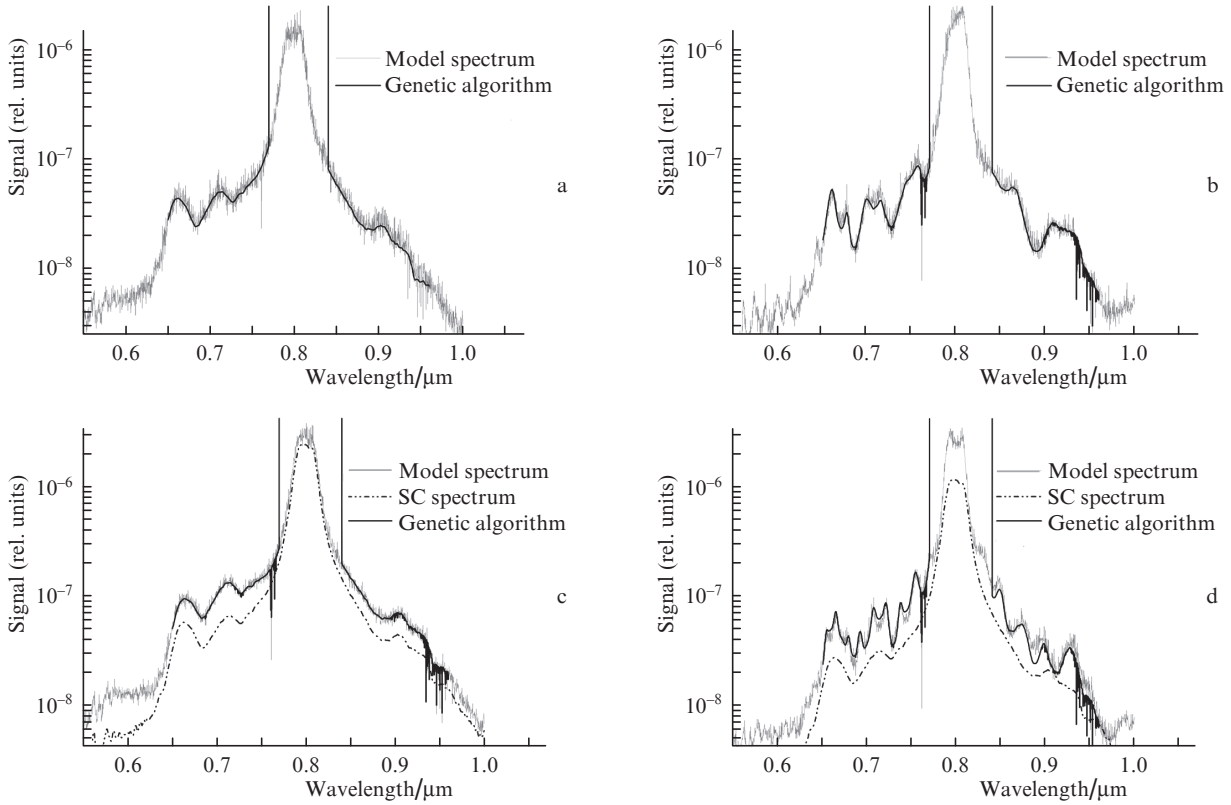

Figure 4. Fitting of the scattering spectra obtained by the genetic algorithm to the model spectra obtained by the Monte Carlo method for modal particles with the radius (a) 1, (b) 1.5, (c) 0.5 and (d) 2 μm.

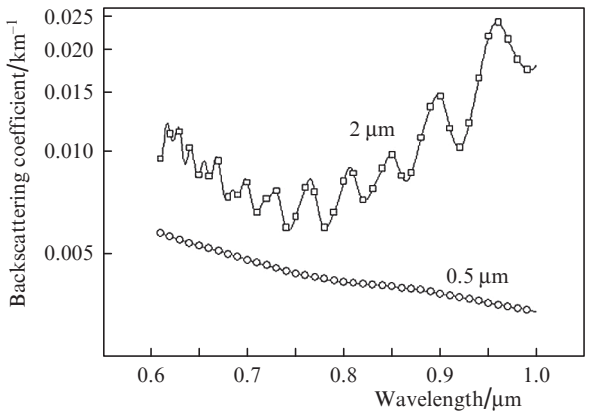

Figure 5. Spectral dependence of the backscattering coefficient for a model medium with particle radius of 0.5 and 2 μm.

of the backscattering coefficient for the medium with the particles of 0.5 and 2 μm radius (Fig. 5).

The curves in Fig. 5 vividly illustrate the backscatter coefficient variation in the wavelength range of 0.6–1 μm: it changes two-fold for the particles of 0.5 μm radius, and five-fold for the particles of 2 μm radius (at equal concentration of particles).

In Fig. 6, the experimental backscattering spectra are compared with the results of modelling. The scattering spectra of SC radiation are obtained with the use of the above-discussed genetic algorithm, and, following the minimisation condition (7), these spectra are compared with the experimental spectra of SC backscattering, which allows reconstruction of the particle size distribution function for aerosol.

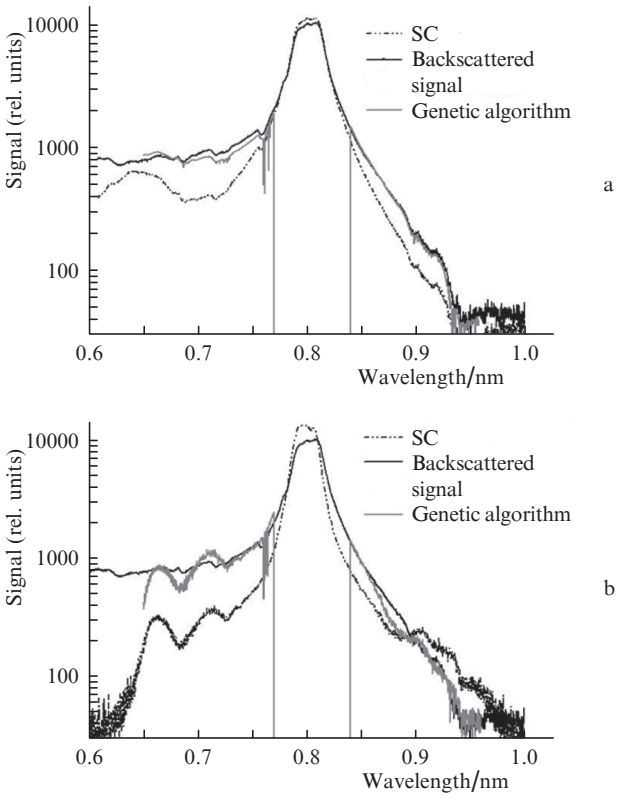

Figure 6. Comparison of experimental spectra of the backscattered signal with model spectra (fitting with the use of the genetic algorithm).

In the first case (Fig. 6a), a satisfactory solution is obtained for the mode of 0.498 μm radius, in the second case (Fig. 6b)

the modes with radiuses of 0.27 and 0.6 μm are reconstructed. We should remind that the modal size of aerosol particles in the experiment was 1 μm.

In the first case, in reconstruction of the distribution function, we used as the SC spectrum a spectrum recorded at the path end and relevant to this experiment. A rather good result was obtained for the case when one mode is reconstructed, whilst the weight of the other one is close to zero. In the second case, a spectrum averaged over multiple realisations was used as the SC spectrum. An attempt was made to take into account simultaneously the half-width of the particle size distribution function and the background disturbances conditioned by scattering of SC spectral components in the atmosphere up to the volume of aerosol scattering. Certain errors arise in reconstruction of the original spectrum of the particle size distribution: two modes are reconstructed in the particle distribution, with the most probable particle radius value shifted to 0.6 μm.

5. Discussion of results

An example is given of the possibility of using the genetic algorithm in the problem of reconstructing the distribution modes with a half-width up to 0.01 μm for the analysis of lidar signals with a wide spectrum. Such narrow distributions correspond to the artificial aerosol sources. Testing the results obtained by means of the genetic algorithm has been performed using the data of numerical experiment on solving the direct problem by the Monte Carlo method.

The genetic algorithm was used to solve the inverse problem of reconstruction of the particle size distribution functions with the particle radius of 0.5, 1, 1.5 and 2 μm, on the basis of experimental results of lidar sensing of artificial aerosol formation on a short atmospheric path.

Reconstruction of the distribution function mode on the basis of the genetic algorithm using the experimental spectra of backscattered SC radiation gives satisfactory results – it is accurate enough in model problems, the signal-to-noise ratio on average in the spectrum range is equal to 30. In some cases this ratio reaches a minimum of 0.5 at an insignificant (about 0.001–0.01 μm) deviation of the radius of the reconstructed mode from a true value.

It is worth mentioning the case of reconstruction of bimodal distribution of aerosol particles in sizes instead of the expected single-modal one. This result is a consequence of incorrect consideration of the experiment specifics. From our viewpoint, we observe here a manifestation of the influence of the angular dependence in spectral distribution of SC radiation on the geometrical form-factor (the relation between the divergence angles of probe radiation and the field-of-view of the telescope), the magnitude of which, provided that the field-of-view of the telescope is constant, depends on the wavelength and position of the point of filamentation on the sensing path. Recall that the position of the point of filamentation and, consequently, of the point of generation of the conical SC emission was not fixed on the real path in this full-scale experiment and was varied from experiment to experiment. Additional numerical experiments have shown that the selection of a lidar scheme requires taking into account not only the endoatmospheric position of the source of spectral signals of sensing (i.e. positioning of the point of filamentation [8]), but also the spectral dependence of the form-factor of the receiving telescope.

In our subsequent studies, we plan to investigate the possibility of reconstructing the spectra of size distributions for real atmospheric aerosol formations (lightweight, advective and radiative fogs). It is also necessary to carry out a series of experimental studies as to the effect on reconstruction accuracy of various sources of background and noise components and to study the conditions of controlling the positioning of the point of filamentation and, consequently, the point of SC generation on the sensing path. It is obvious that such an effect would result from taking into account the signals from molecular components of atmosphere, background aerosol and its characteristics, and engineering parameters of the sensing system.

This numerical experiment can be used for further development of methods and tools in solving urgent problems of environmental monitoring by means of a femtosecond lidar, and in particular, for measuring and analysis of factory emissions and other pollutants.

Acknowledgements. This work was performed in the framework of the Programme for Basic Research of the Presidium of the Russian Academy of Sciences 'Extreme Light Fields and Their Applications' and the RF President's Grant Council (State Support of Scientific Schools of the Russian Federation Programme, Grant No. NSh-4714.2014.5 'Laser Sensing of The Atmosphere and The Ocean').

References

1. http://www.teramobile.org/publis.html.
2. Wille H., Rodrigues M., Kasparian J., et al. *Eur. Phys. J. Appl. Phys.*, **20**, 183 (2002).
3. Petit Y., Henin S., Kasparian J., Wolf J.-P. *Appl. Phys. Lett.*, **97**, 021108 (2010).
4. Maioli P., Salamé R., Lascoux N., Salmon E., Béjot P., Kasparian J., Wolf J.-P. *Opt. Express*, **17** (6), 4726 (2009).
5. Trapani P. Di, Valiulis G., Piskarskas A., Jedrkiewicz O., Trull J., Conti C., Trillo S. *Phys. Rev. Lett.*, **91**, 093904 (2003).
6. Conti C., Trillo S., Trapani P. Di, Valiulis G., Piskarskas A., Jedrkiewicz O., Trull J. *Phys. Rev. Lett.*, **90**, 170406 (2003).
7. Ettoumi W., Bjot P., Petit Y., Loriot V., Hertz E., Faucher O., Lavorel B., Kasparian J., Wolf J.-P. *Phys. Rev. A*, **82**, 033826 (2010).
8. Bagayev S.N., Matvienko G.G. (Eds) *Femtosekundnaya atmosfernaya optika* (Femtosecond Atmospheric Optics) (Novosibirsk: Izd-vo SO RAN, 2010).
9. Banakh V.A., Belov V.V., Zemlyanov A.A., Krekov G.M., Lukin V.P., Matvienko G.G., Nosov V.V., Sukhanov A.Y., Falits A.V. *Rasprostranenie opticheskikh voln v neodnoronykh sluchainykh nelineinykh sredakh* (Optical Wave Propagation in Inhomogeneous Random Nonlinear Media) (Tomsk: Izd-vo IOA SO RAN, 2012) p. 402.
10. Kandidov V.P., Shlenov S.A., Silaeva E.P., Dergachev A.A. *Opt. Atmos. Okeana*, **23** (10), 873 (2010).
11. Golubtsov I.S., Kandidov V.P., Kosarev O.G. *Opt. Atmos. Okeana*, **14** (5), 335 (2001)
12. Apeksimov D.V., Geints Yu.E., Zemlyanov A.A., Kabanov A.M., Matvienko G.G., Oshlakov V.K., Stepanov A.N. *Opt. Atmos. Okeana*, **23** (11), 1006 (2010).
13. Bagaev S.N., Geints Yu.E., Zemlyanov A.A., Kabanov A.M., Matvienko G.G., Pestryakov E.V., Stepanov A.N., Trunov V.I. *Opt. Atmos. Okeana*, **20** (5), 413 (2007).
14. Geints Yu.E., Zemlyanov A.A., Krekov G.M., Matvienko G.G. *Opt. Atmos. Okeana*, **23** (5), 325 (2010).
15. Geints Yu.E., Zemlyanov A.A., Krekov G.M., Krekova M.M., Matvienko G.G. *Opt. Atmos. Okeana*, **19** (10), 827 (2006).
16. Krekov G.M., Sukhanov A.Y. *Opt. Atmos. Okeana*, **24** (9), 754 (2011).
17. Krekov G.M., Krekova M.M., Sukhanov A.Y. *Opt. Atmos. Okeana*, **22** (5), 482 (2009).

18. Krekov G.M., Krekova M.M., Sukhanov A.Y. *Opt. Atmos. Okeana*, **22** (7), 661 (2009).
19. Krekov G.M., Krekova M.M., Sukhanov A.Y. *Opt. Atmos. Okeana*, **22** (8), 795 (2009).
20. Krekov G.M., Krekova M.M., Sukhanov A.Y. *Opt. Atmos. Okeana*, **22** (9), 862 (2009).
21. Babin A.A., Kiselev A.M., Sergeev A.M., Stepanov A.N. *Kvantovaya Elektron*., **31** (7), 623 (2001) [*Quantum Electron*., **31** (7), 623 (2001)].
22. Zuev V.E., Naats I.E. *Obratnye zadachi lazernogo zondirovaniya atmosfery* (The Inverse Problems of Laser Sensing of The Atmosphere) (Novosibirsk: Nauka, 1982).
23. Krekov G.M. *Opt. Atmos. Okeana*, **23** (1), 47 (2010).
24. Mikhailov S.A. *Opt. Atmos. Okeana*, **7** (2), 265 (1994).
25. Arshinov M.Y., Belan B.D., Davydov D.K., Krekov G.M., Fofonov A.V., Babchenko S.V., Inoue G., Machida T., Maksutov Sh.Sh., Sasakawa Motoki., Shimoyama Ko. *Opt. Atmos. Okeana*, **25** (12), 1051 (2012).
26. Hess M., Koepke P., Schult I. *Bull. Am. Met. Soc.*, **79** (5), 831 (1998).
27. Virolainen Ya.A., Polyakov A.V., Trofimov Yu.M. *Izv. Ros. Akad. Nauk, Ser. Fiz. Atmos. Okeana*, **40** (2), 255 (2004).
28. Hoffman H.E., Roth R. *Meteorol. Atmosp. Phys.*, **41**, 247 (1989).
29. Zuev V.E., Krekov G.M. *Opticheskie modeli atmosfery. Sovremennye problemy atmosfernoi optiki* (Optical Models of The Atmosphere. Modern Problems of Atmospheric Optics) (Leningrad: Gidrometeoizdat, 1986) Vol. 2.